A Testing Methodology for Performance-Based Specification

A Testing Methodology for Performance-Based Specification

W. J. McCarter [1] *

B. Suryanto [1]

H. M. Taha [1]

S. Nanukuttan [2]

P. A. M. Basheer [3]

[1] Heriot Watt University,
School of Energy, Geoscience, Infrastructure and Society,
Edinburgh, EH14 4AS,
U.K.

[2] Queen's University,
School of Planning, Architecture and Civil Engineering,
Belfast, BT7 1NN,
U.K.

[3] University of Leeds,
School of Civil Engineering,
Leeds LS2 9JT, UK

* Corresponding Author: E-mail: w.j.mccarter@hw.ac.uk
Phone: +44-131-451-3318
Fax: +44-131-451-4617

A Testing Methodology for Performance-Based Specification

Satisfactory guidelines for ensuring adequate reinforced concrete durability can only be developed by monitoring concrete performance under a range of field exposure conditions over an extended period of time. Only then can there be a move from prescriptive durability specifications (minimum grade, maximum water-binder ratio, and minimum cement content) to performance-based methods. The situation is also made more complex by the range of cements now available - BS EN 197 defines a total of 27 products in the family of common cements. Implementation of both design for durability and performance-based standards and specifications are limited by the lack of rapid, simple, science-based test methods for characterizing the transport properties and deterioration resistance of concrete. This paper presents an overview of performance-based specification and developments in the application of electrical property measurements as a candidate testing methodology in evaluating the relative performance of concrete mixes. The technique lends itself to in-situ monitoring thereby allowing measurements to be obtained on the *as-placed* concrete.

Keywords: concrete, durability, performance, resistivity, formation factor, testing

Introduction

A state of the nation report (New Civil Engineer, 2000) graded the quality of the UK's infrastructure from B (fair) to D (poor) with an overall grading of C (average). A similar situation exists in the US, where the ASCE Report on America's Infrastructure (ASCE, 1998) estimated a five-year total investment need of US$1.3 trillion just to reinstate roads, bridges and other infrastructure systems to good serviceable life; in 2005, this investment need had risen to US$1.6 trillion. Further to this, the average state of America's infrastructure was given a Grade D (Poor); as a specific example, in excess of 40% of 500,000 highway bridges are rated as structurally deficient or functionally obsolete and some US$100 billion is the

estimated requirement to eliminate the current backlog of bridge deficiencies and maintain repair levels (Swamy, 2008).

Considering reinforced concrete structures, the initiation and propagation stages of deterioration result from a complex interaction of physical, chemical and electrochemical phenomena. The rate at which a particular structure deteriorates depends on many factors and evaluating the performance of reinforced concrete requires numerous data inputs, in particular, the response of the concrete to the changing micro-environment in the vicinity of a specific structural element or part of a structure. As it is the concrete cover-zone which protects the steel reinforcement - and therefore provides the first line of defence against the environment - it is understandable that considerable attention is directed towards assessing the performance of this zone (Long, Henderson and Montgomery, 2001; Basheer and Nolan, 2001; Basheer and Barbhuiya, 2010). The protective properties of the cover-zone are a major factor with regard to the in-service performance of the structure, likely deterioration rates for a particular exposure condition and compliance with specified design life. It is permeation processes such as diffusivity and sorptivity which are important and there clearly exists a need to study and determine quantitatively those near-surface characteristics of concrete which promote the ingress of gases or liquids containing dissolved contaminants.

Regarding concrete durability, European Standard BS EN206 (BSI, 2013a) deals with durability on the basis of a prescriptive, deem-to-satisfy approach by specifying minimum grade, minimum binder content and maximum water-binder ratio for a series of well-defined environmental classes. Interestingly, section 5.3.3 of this code allows for performance-related methods and defines concrete on the basis of an *equivalent durability procedure* (EDP); further detail on the EDP is presented in PD CEN/TR 16563 (BSI, 2013b). However, in order to fully implement a performance-based strategy requires,

(1) long-term experience of local materials and practices and on a detailed knowledge of the local environment;
(2) test methods based on approved and proven tests that are representative of actual conditions and have approved performance criteria; and,
(3) analytical models that have been calibrated against test-data representative of actual conditions in practice.

Performance Testing

Although attempts have been made to introduce performance-based specifications, the lack of reliable, consistent and standardised test procedures for evaluating concrete performance has hindered its widespread implementation. Furthermore, there is also an intense need to evaluate the concrete as early as possible; the sooner information is obtained about the early-age properties of any given batch of concrete, the sooner adjustments can be made to the materials, proportions or processes for subsequent concrete placement, and the sooner remedial measures can be initiated on the concrete already installed or construction practices altered (e.g. extended curing). Early-age testing is useful in this regard as the consequences of unsatisfactory concrete discovered at a later stage becomes expensive. The term *identity testing* is used in BS 8500-1 (BSI, 2016) to describe testing to validate the identity of the mix. Identity testing attempts to verify some key characteristic of the concrete that relates to the desired performance and could take the form of a slump, flow, density, strength, water-content or some non-destructive or in-place method.

According to BS EN1990 (BSI, 2005), a reinforced concrete structure is designed in such a way that *'deterioration over its design working life does not impair the performance of the structure below that intended, having due regard to its environment and the anticipated level of maintenance'*. It is evident that consideration of a maintenance strategy forms an

integral part of the structural design process. Implicit within this process is a consideration of adequate monitoring procedures, together with an appropriate level of inspection for the particular structure. As noted above, cover-zone transport mechanisms, their variation through the cover-zone, cyclic wetting/drying characteristics and temporal changes in properties all influence reinforced concrete performance and durability. In-situ monitoring of cover-zone concrete – in both the spatial and temporal domains - could thus assist in making realistic predictions as to the in-service performance of the structure; likely deterioration rates for a particular exposure condition, compliance with the specified design life and as an early warning indicator of incipient problems. Fig. 1 (adapted from Tutti, 1982) highlights the usefulness of in-situ monitoring of concrete performance during the life of the structure which can be divided into three stages: an initial stage which represents the concrete response to the external environment, a second stage which represents the initiation of the deterioration process (corrosion in this instance) and a third stage where propagation of deterioration occurs.

The specification of the service-life/performance/durability of reinforced concrete by means a single parameter is the *holy grail* of the engineer and hence a subject of intense research interest (see, for example, Neithalath, Persun, and Manchiryal, 2010; Muigai, Moyo and Alexander, 2012; Spragg et al, 2013; Andrade, d'Andrea and Rebolledo, 2014; Nganga, Alexander and Beushausen, 2015; Merioua, Bezzar and Ghomari, 2015). The challenges posed by a performance-based testing and specification approach to improve service life of concrete structures have been acknowledged (Beushausen and Fernandez-Luco, 2015). It is set against this background that the work presented examines the use of the intrinsic electrical properties of cementitious materials (resistivity in the current work) as a potential candidate testing methodology in assessing concrete performance. Moreover, as the electrical resistivity

of the concrete surrounding the rebar controls the magnitude of the corrosion current, it makes this parameter an important factor in the overall corrosion dynamics.

The work detailed specifically highlights the development of a testing methodology for in-situ monitoring of the as-placed concrete, which can be undertaken from initial gauging, through setting and throughout the long-term hardening process. In addition, the combination of concrete resistivity measurements and the calculated pore-fluid resistivity could be used to rank the durability performance of concrete mixes.

Electrical Property Measurements

From an electrical point of view, concrete can be regarded as a composite comprising non-conductive aggregate particles embedded in an ionically conducting cementitious matrix, with conduction occurring primarily through the continuous water-filled, pore-network. As a consequence, the electrical properties of concrete are directly related to setting and hardening processes, so its measurement could be of practical significance in assessing the durability of concrete. In addition, as the hydration process will alter the pore system (e.g. pore tortuosity, pore connectivity) beyond the standard curing period, this will result in time-variant microstructural - hence electrical property - changes.

The electrical resistivity of a material is a fundamental electrical property and is equal to the resistance, in ohms, between opposite faces of a unit cube of that material. Hence, if R is the bulk resistance of a prismatic sample of concrete placed between two electrodes of area A (cm^2), separated by a distance L (cm), then its bulk resistivity, ρ, is given by,

$$\rho = \left(\frac{RA}{L} \right) \text{ Ohm-cm} \quad (\Omega\text{cm}) \qquad (1)$$

Conventional treatment of resistivity data - saturated rocks in this instance - has been to utilise the formation factor *F* (Archie, 1942; Atkins and Smith, 1961) which is defined as

the ratio of bulk resistivity, ρ, of the saturated rock to the resistivity of the saturating liquid, ρ_p. The formation factor is then related to the rock porosity, φ, through the relationship,

$$F = \frac{\rho}{\rho_p} = a\varphi^{-m} \tag{2}$$

where the exponent *m* is the cementation exponent, and is related to the tortuosity and connectivity of the pore network within the rock and *a* is a correction factor which is valid over a particular range of porosities, φ. A wide range of values have been reported for *m* and *a* for different rock and sediment formations, with *a*, typically, in the range 0.4–2.5 and *m* = 1.2–2.5 (Worthington, 1993; Khalil and Santos, 2009). Values of *m* and *a* are characteristic for a given porous rock formation and are determined empirically.

Provided that the solid phase can be regarded as an insulator in comparison to that of the interstitial aqueous phase, diffusion and resistivity of a saturated porous system are connected through the relationship (Atkinson and Nickerson, 1984; Scherer, Valenza and Simmons, 2007),

$$\frac{\mathrm{D}}{\mathrm{D_O}} = \frac{\rho_\mathrm{p}}{\rho} = \frac{1}{\mathrm{F}} \tag{3}$$

where D is the diffusion coefficient of an ion in the porous material, D_o the free solution diffusion coefficient of the ion.

The work detailed above indicates that the electrical resistivity of concrete provides an indirect measure of the capillary pore network (continuity, tortuosity) which is a key property of concrete to resist the permeation of a fluid. In order to fully exploit electrical property measurements in assessing the relative performance of different concrete mixes, however, the resistivity of the pore-fluid, ρ_p, needs to be estimated. This is particularly relevant when supplementary cementitious materials (SCM) are used as these materials alter the

concentrations of Na^+, K^+ and OH^- within the interstitial aqueous phase in comparison to a plain Portland cement concrete (Shi, Stegeman and Caldwell, 1998). In order to evaluate the resistivity of the pore-fluid, pore expression techniques can be used to *squeeze* the pore-fluid out of the hardened cement paste; however, this is impractical for a variety of reasons, not least because it complicates the testing procedure. The pore-fluid resistivity could be estimated from the ionic concentrations predicted from the chemical composition of the binder. For example, the model of Taylor (Taylor, 1987) predicts the concentration of various ionic species in the pore solution based on the cement composition and degree of hydration. From the estimated concentrations of the ions, it is then possible to evaluate the resistivity of the pore-fluid. In this work, the model developed by Snyder, Feng, Keen, and Mason (2003) and Bentz (2007) is used to estimate the resistivity of the pore fluid.

Experimental

In order to investigate to applicability of electrical measurements to monitor the short- and long- term performance of concrete, developments were made on two fronts (a) electrical measurements on concretes taken during the initial 24-hours after casting, and (b) electrical measurements taken during long-term hardening and cyclic ponding up to 350 days hydration. Different electrode configurations were used for each regime and described below. In the current work, testing was carried out in a temperature controlled laboratory (22°C±1°C, 55%±5%RH).

Materials

The concrete mixes used within the experimental programme are presented in Table 1 with a crushed granite aggregate used throughout together with a mid-range water reducer/plasticiser (SikaPlast 15RM). Table 1 also presents the 28-day and 56-day concrete compressive strengths, denoted f_{28} and f_{56}, respectively, which were determined on 100mm cubes cast at the same time as the slabs detailed below (6 per mix). The oxide analysis of the cementitious materials is presented in Table 2.

The range of mixes, in terms of binder-content, binder composition and water-binder ratio, would satisfy minimum requirements specified in BS 8500-1 (BSI, 2016) for environmental exposure classes XC (corrosion induced by carbonation), XS (corrosion induced by chlorides from sea-water) and XD (corrosion induced by chlorides other than sea-water e.g. deicing salt) for an intended working life of 100 years, with 50mm cover-to-steel.

Testing over Initial 24-hours

Concrete samples were compacted into plastic (non-conductive) cuboidal moulds of internal dimensions 150mm×150mm×150mm. A pair of stainless-steel electrodes, 2.4mm diameter, were embedded into each concrete sample (three samples per mix) with a center-to-center spacing of 75mm and embedded to a depth of 75mm. The electrodes were held securely in position using a PVC former placed across the top of the cube mould. Embedding the electrodes in this fashion ensured intimate contact with the sample and reduced any interference with the natural distribution of aggregate. A thermistor was also embedded centrally within each cube to allow internal temperature measurements. The top surface of the cell was covered to prevent evaporation; the electrodes were connected to an LCR meter with electrical resistance measurements taken on a 4 minute cycle throughout the initial 24-hours

after gauging. In order to avoid problems with electrode-polarization, the frequency of the applied field was 100kHz.

Testing during Long-Term Hardening

Samples (3 per mix) for this stage of the experimental programme were cast as 250×250×150mm (thick) slabs in steel formwork with the 250×250mm face cast against the formwork used as the working face. To facilitate ponding, an integral 20mm dyke was cast around the working face. On demoulding at approximately 24-hours, each specimen was wrapped in damp hessian and placed in a heavy-duty polythene bag which was then sealed. The specimens were then left in a laboratory for a period of 27-days. At this time, the four vertical faces and the as-cast face of the specimens were painted with two coats of an epoxy-based sealant and left in a laboratory environment. After approximately 7-days, all samples were ponded with water for a period of 24-hours. This ensured the surface region of all specimens was in a similar saturated state. Samples were then allowed to dry for a further 7-days before being subjected to a cyclic ponding regime viz. 1-day wetting followed by 6-days drying.

In this part of the study, electrical measurements were obtained utilizing a multi-electrode array (McCarter, Chrisp and Starrs, 2011) which was embedded within the sample at the time of casting. This arrangement allowed monitoring of the spatial distribution of both electrical resistance and temperature. In summary, the array comprised six electrode-pairs and four thermistors mounted on a PVC former, with the former being secured onto two, 15mm diameter steel bars; the cover-to-steel was 50mm. Each electrode comprised a 1.6mm diameter stainless steel rod, sleeved with insulation to expose a 10mm tip; the centre-to-centre spacing between the electrodes was 10mm. With this arrangement, the electrode-pairs were positioned at 10, 20, 30, 40, 50 and 75mm from the concrete surface (see Fig. 2(a)). The

electrode array was positioned at the plan centre of each slab with wiring from the embedded array ducted out of the slab and terminated with a multipole D-connector. On demoulding at 24-hours, electrical resistance and thermistor (temperature) measurements on the array were then taken on a 12-hour cycle using a multiplexing system (see Fig. 2(b)) with testing extending up to 350 days.

Calibration of Electrode Arrangements

The resistivity of the concrete was evaluated by multiplying the resistance measured across the electrodes by a calibration factor, denoted k , as shown in equation (4) below. As the electrical field between the electrodes is non-uniform, the geometrical factor A/L in equation (1) is not readily calculable and was obtained by calibrating the electrode arrangement in liquids of know resistivity. This was undertaken for the electrode arrangement used in both the cubes (24-hour hydration study) and slabs (long-term hardening study). The measured resistance, R (ohms), across the electrodes was then converted to resistivity, ρ (in Ωcm), through the relationship,

$$\rho = kR \quad \Omega\text{cm} \tag{4}$$

The calibration factor, k was obtained as 5.77cm for the cube specimens and for each electrode-pair on the array k was 2.41cm.

Results and Discussion

Due to the considerable amount of data collected, only a selection of results are presented for illustrative purposes and, for reasons of clarity, only selected measurement points are highlighted on the figures (although graphs presented were drawn through all measurement points).

Response during initial 24-hours

Fig. 3(a) presents the resistivity, ρ, during the initial 24-hours for the PC concrete mixes in Table 1; also shown in this Figure is the ρ-time response for the w/b = 0.35 concrete mix without the addition of plasticiser. The curves can be divided into two distinct regions: an initial region of decreasing resistivity followed by a region of increasing resistivity over the remainder of the 24-hour test period. However, it is evident that the time over which these regions occur, the absolute values of resistivity within each region and the rate of change of resistivity within each region depends on the w/b ratio and addition of plasticiser.

During mixing, dissolution of ions from the cement grain surfaces takes place, with the different mineralogical phases and calcium sulphate contributing to the pore-solution chemistry. The interstitial aqueous phase contains, primarily, Na^+, K^+, Ca^{2+}, SO_4^{2-} and OH^- which increases with time and, as conduction will be primarily electrolytic in nature, will result a decrease in resistivity. The period of decreasing resistivity extends over 0-1.5 hours for the concrete (w/b = 0.35) without plasticiser, whereas for the same concrete with plasticiser this period has increased to 0-2.5 hours indicating a slower dissolution process, which is a similar time-scale for the higher w/b ratio concrete (0.65); however, the w/b= 0.65 concrete achieves a lower resistivity simply as a result of the higher volumetric water content of this mix. A period of increasing resistivity follows which is taken to imply an increase in rigidity of the concrete. As the cement paste hydrates, its porosity decreases with the pore network becoming more tortuous, constricted and disconnected as a crystalline network is formed. As conduction is electrolytic via the continuous capillary pores, this will result in an increase in resistivity of the concrete. Regarding the PC concrete (w/b = 0.35), it is also evident that the resistivity of the concrete without plasticiser increases at a faster rate than the concrete with plasticiser highlighting that the plasticiser is having a retarding effect on the

hydration process. The retarding effect results in resistivity values that are similar to the w/b = 0.65 PC concrete over the initial ~15 hours

The influence of the SCM's on early hydration can be seen in Figs. 3(b) and (c). As with the PC concretes, the resistivity decreases due to increasing ionic concentration within the water phase although the absolute values of resistivity are higher due to the reduced PC content of these mixes(hence lower ionic concentrations) and *inert* nature of the SCM during the early stages of hydration which is acting as a filler material. During the period after the resistivity minimum, the resistivity increases albeit at a slower rate than the PC concrete; as before, the retarding effect of the plasticiser results in the resistivity vs time response being similar for both w/b ratios.

Response during period 24-hours – 350 days

Preliminaries

Fig. 4 presents the resistivity, ρ, for the electrodes positioned at 10, 20, 30 and 75mm from the surface for the PC concrete mix (w/b=0.65) with data presented between 100 and 200 days after casting. Note that for reasons of clarity, only every 5^{th} measurement point is highlighted. The influence of the cyclic wetting/drying regime on the concrete resistivity is clearly evident for the electrode-pairs positioned 10mm and 20mm from the surface, with periods of wetting resulting in a decrease in resistivity and drying accompanied by an increase in resistivity. The electrode-pair positioned at 75mm, however, displays a continual increase and is not influenced by wetting/drying at the concrete surface. Similar responses were obtained for the other concrete mixes and it is for this reason that only measurements from the electrode-pair positioned at 75mm from the exposed surface, and still within the near-surface region, are presented and discussed below. The electrical measurements

obtained at 75mm will thus reflect cement hydration, pozzolanic reaction and microstructural development.

Resistivity/Time response

Fig. 5(a) presents the resistivity for concrete mixes with w/b=0.35 over the initial 4-weeks after demoulding i.e. during the curing period. The resistivity of all mixes display a continual increase although the influence of the SCM's on resistivity is also evident. For periods <3 days, the PC concrete displays a higher resistivity than the FA/35 and GGBS/65 mixes and reflects the initial slower reaction of these systems. However, for periods >3-days, the resistivity of the GGBS/65 concrete achieves higher values than the PC concrete whereas for the FA/35 concrete, this effect does not occur until approximately 15 days. Similar trends are observed in Fig. 5(b) for concrete mixes with w/b=0.65 although the resistivity of the FA/35 mix only achieves higher values than the PC mix at periods in excess of 28-days. It is also apparent that there is an inverse relationship between w/b ratio and resistivity.

Figs. 6(a) and (b) display the resistivity at 75mm from the surface from 7-days up to approximately 350 days for 0.35 and 0.65 w/b ratios (Note: again, for clarity, only every 20th measurement point is highlighted on these curves). The influence of SCM's on the resistivity is now clearly evident from these Figures; at the end of the test period, the resistivity of the FA/35 and GGBS/65 mixes are almost an order of magnitude higher than the PC mix, at both w/b ratios. The increase in resistivity for both the GGBS and FA concretes reflects the on-going reactivity of the SCM's and pore structure refinement during the post-curing period.

The temporal increase in resistivity for the concretes presented in Fig. 6 can be represented by the equation of the form,

$$\rho_t = \rho_{ref}\left(\frac{t}{t_{ref}}\right)^n \qquad (5)$$

where, ρ_t is the resistivity at time, t (in days); ρ_{ref} is the resistivity at a reference time, t_{ref}, and *n* could be regarded as an *aging* exponent which will be related to hydration and pozzolanic reaction. The reference time for the current work is taken as 28-days, hence t_{ref} = 28-days and the respective resistivity at 28-days, ρ_{ref}, obtained from Fig. 5. Best-fit curves to the data are plotted on Figure 6(a) and (b) (solid lines) through the measurement points with the fitting equations presented on these Figures. It is interesting to note that the aging exponent, *n*, would appear to be virtually independent of w/b ratio and is binder specific. This could be explained by the fact that the influence in of the w/b ratio is accounted for in the 28-day resistivity, ρ_{ref}.

Although the equations on these Figures were developed on the best-fit line to all the data points for a particular w/b ratio (i.e. over 700 measurement points), a curve could be evaluated from fewer measurements, which has obvious practical implications. For example, Figs. 7(a) and (b) present the best-fit curves (solid lines) based on resistivity measurements at 3 measurement points (7, 28 and 56 days) using the same reference time of 28-days. For comparative purposes, the best-fit curves based on all the measurement points on Fig. 6 are also presented on Fig. 7 (dashed lines).

Whilst the resistivity versus time response can be used to assess the rate of change of resistivity for the different concrete mixes, on its own, however, resistivity cannot be used as a measure of their relative durability performance. As noted earlier, the resistivity of concrete is not only dependant on the pore structure but also pore fluid resistivity which must be considered. This aspect is discussed below.

Towards a Performance-Based Index

From the definition of formation factor (F) in equation (2) above, and its relationship with diffusivity through equation (3), concretes could be ranked in terms of their resistance to

ionic penetration using the parameter, F. However, the formation factor requires a knowledge of the pore-water resistivity. A straightforward procedure for estimating pore-water resistivity from the concentrations of Na^+, K^+ and OH^- ions in the pore-water has been developed (Snyder, Feng, Keen and Mason, 2003; Bentz, 2007). In their work, for a particular degree of hydration, the concentrations of Na^+ and K^+ are computed from the binder composition (Table 2) and it was assumed that 75% of the Na_2O and K_2O will be released into the pore-water. The concentration of OH^- is then deduced from the electro-neutrality condition. Using the equivalent conductivity of each ion, these data are then used to compute the pore solution electrical resistivity, ρ_p, which is presented in Fig. 8.

Table 3 presents the computed F values for each concrete mix in Table 1 at both 28-days (F_{28}) and 56-days (F_{56}); in calculating ρ_p, an average degree of hydration of 80% has been assumed throughout for each binder type (although it is evident from Fig. 8 that hydration does not have a significant influence on pore fluid resistivity over the range 50%-95% hydration). With reference to Table 3, decreasing the w/b ratio from 0.65 to 0.35 results in a fivefold (approximately) increase in F for each mix. Moreover, the beneficial effect of the FA and GGBS is clearly evident, particularly at longer time-scales. Although these materials may not necessarily create concretes of lower porosity than their PC counterparts, it is of a more disconnected and tortuous in nature (Li and Roy, 1986; Lu, Landis and Keane, 2006). It is interesting to note that whilst the GGBS/65 concrete displays the highest resistivity, when the resistivity of the pore-water is considered, it is out-ranked by the FA/35 concrete in the longer-term.

When equation (3) above, is combined with equation (5), the *instantaneous* diffusion coefficient at time, t, $D_i(t)$, of a particular ionic species (e.g. Cl^-) could be approximated as,

$$D_i(t) = D_o \frac{\rho_p}{\rho_{ref}} \left(\frac{t}{t_{ref}}\right)^{-n} \qquad (6)$$

Consider the FA concrete with w/b=0.35. If, over the test period, an *average* degree of hydration of 80% is assumed then, from Fig. 8, the resistivity of the pore-water, ρ_p, is evaluated as 8.31 ohm-cm; taking the self-diffusion of the chloride ion (Cl^-) in pure water, D_o, as 1.84×10^{-9} m^2/s (Li and Gregory, 1974; Shackleford and Daniel, 1991), then, from Fig. 5(a) and equation (6) above, the time-dependant, instantaneous diffusion coefficient, $D_i(t)$, could be approximated by the relationship,

$$D_i(t) = 1.63 \times 10^{-12} \left(\frac{t}{28}\right)^{-1.06} \; m^2/s \qquad (7)$$

It must be stressed that $D_i(t)$ represents the diffusion coefficient at time, t, and not the effective (or apparent) diffusion coefficient, D_{eff}, normally referred to in the literature. D_{eff} is generally obtained from the error function solution to the chloride profile obtained from dust drillings taken through the cover-zone and thus represents the integrated, or time-averaged, diffusion coefficient. Hence, if D_{eff} values are used to make predictions as to future chloride ingress they will tend to underestimate the time to activation of corrosion.

It is accepted that the evaluation of the resistivity of the pore-water is, at best, approximate, however, considering the extremely wide variation in published values for diffusion coefficients for concretes with and without SCM's (Bamforth, Price and Emerson, 1997), this methodology could be developed a means for estimating the diffusion coefficient and ranking the performance of different concretes.

Conclusions and Concluding Comments

The work detailed has presented developments in the application of the electrical properties of concrete as a candidate testing methodology in assessing both the early hydration characteristics (<24-hours) and the long-term performance of concrete. This was achieved by

using electrical resistivity measurements in combination with the pore-fluid resistivity evaluated from the oxide composition of the cementitious materials.

The following conclusions can be drawn:

1. Resistivity measurements taken during the early hydration period (24-hours) indicated that the response comprised two distinct regions – a initial region (up to ~3.0 hours) of decreasing resistivity resulting from dissolution processes and increasing ionic concentration within the interstitial aqueous phase followed by a region of increasing resistivity resulting from setting and the increase in rigidity of the concrete.
2. Further to conclusion 1 above, the addition of SCM's result in higher resistivity values during the initial region and is attributed to the reduced ionic concentrations within the aqueous phase and filler effect of the SCM. Furthermore, resistivity measurements clearly show that the addition of plasticiser has a mild retarding effect on the early hydration processes and, as such, the testing methodology could be used to study the influence of chemical admixtures on setting and hardening.
3. Further to conclusion 1 above, during the period of increasing resistivity, the resistivity of the PC concrete increases at a faster rate than those concretes containing SCMs and reflects the slower reaction during the initial stages of hydration.
4. Over the period 1day up to ~350 days, the resistivity of concrete increases with time due to the ongoing hydration and pozzolanic processes. In the short-term the resistivity of concretes containing SCM's is lower than the respective PC mix due to a slower reaction; however, in the longer term, the resistivity of the FA and GGBS concretes displays a more marked increase that that of the PC concretes and attributed to a more disconnected and tortuous capillary pore network.

5. Through the use of an ageing factor, a relationship was established to model the development of resistivity with time. The ageing exponent was found to be binder specific and virtually independent of w/b ratio.
6. The term Formation Factor (F) was introduced and used to assess the relative performance of the concrete mixes. In general terms, the higher the F value for the concrete, the better its performance rating; however, work is still required to obtain values, or range of values, for F for concrete classification purposes

The resistivity of concrete is a relatively easy parameter to evaluate and the work detailed above has shown that it can be monitored from initial placing of the concrete, through setting and long-term hardening. In a broader sense, the measurement technology lends itself in-situ monitoring and remote interrogation (McCarter and Vennesland, 2004). The installation of a network of sensors, embedded at critical locations within a concrete structure, could provide continuous, real-time data on the response of the micro-environment within the cover-zone to changing ambient environmental conditions.

Acknowledgements

The work presented formed part of the concrete durability programme into monitoring and improving the performance of structural concrete in bridges and in the development of performance-based testing procedures undertaken for Transport Scotland and the Engineering and Physical Sciences Research Council, UK (Research Grants EP/G025096, EP/G02152X and EP/I005846). Funding from both organisations is gratefully acknowledged. The views expressed in this paper are those of the Authors and not necessarily those of Transport Scotland.

The Authors also wish to acknowledge the support of Hanson Cement (UK) for supplies of materials and the technical support of AmphoraNDT (**www.amphorandt.com**).

References

American Society of Civil Engineers (ASCE) (1998). Report Card for America's Infrastructure. Retrieved from: http://ascelibrary.org/doi/pdf/10.1061/9780784478899 (accessed 12/01/2017)

Andrade, K., d'Andrea, R. and Rebolledo, N. (2014, March). Chloride ion penetration in concrete: The reaction factor in the electrical resistivity model. *Cement and Concrete Composites*. 47, 41-46. doi:10.1016/j.cemconcomp.2013.09.022

Archie, G.E. (1942). The electrical resistivity log as an aid in determining some reservoir characteristics, *Transactions of the American Institute of Mining and Metallurgical Engineers,* 146(1), 54-62. doi.org/10.2118/942054-G

Atkins, E.R. and Smith, G.H. (1961, March 1). The significance of particle shape in formation resistivity factor - porosity relationships, *Society of Petroleum Engineers.* 13, 285-291. doi:10.2118/1560-G-PA

Atkinson, A. and Nickerson, A. K. (1984). The diffusion of ions through water-saturated cement. *Journal of Materials Science*. 19(9), 3068-3078. doi:10.1007/BF01026986

Bamforth, P. B., Price W. F. and Emerson, M. (1997). An international review of chloride ingress into structural concrete. *Transport Research Laboratory*, Contractor Report 359, 162pp. ISBN 0-7277-2928-4

Basheer, P. A. M. and Barbhuiya, S. (2010). Pore structure and transport processes. Chapter 2 in *Concrete durability: A practical guide to the design of durable concrete structures* (M Soutsos, Editor) Thomas Telford Ltd., London. (ISBN 978-0-7277-3517-1)

Basheer, P.A.M. and Nolan E. (2001). Near-surface moisture gradients and in situ permeation tests, *Construction and Building Materials*. 15(2/3), 105-114. doi:10.1016/S0950-0618(00)00059-3

Bentz, D. (2007). A virtual rapid chloride permeability test, *Cement and Concrete Composites.* 29(10), 723-731. doi:10.1016/j.cemconcomp.2007.06.006

Beushausen, H. and Fernandez-Luco L. (Eds). (2015) Performance-based specifications and control of concrete durability, *State-of-the-Art Report RILEM TC 230-PSC.* (ISBN 978-94-017-7309-6).

British Standards Institution (BSI) (2005). BS EN1990:2002+A1:2005 Eurocode – Basis of structural design, *British Standards Institution*, London.

British Standards Institution (BSI) (2013a). BS EN206:2013 Concrete - Specification, performance, production and conformity, *British Standards Institution*, London.

British Standards Institution (BSI) (2013b). PD CEN/TR 16563:2013 Principles of the equivalent durability procedure. *British Standards Institution*, London. ISBN 978-0-580-81434-1.

British Standards Institution (BSI) (2016). BS EN8500-1:2015+A1:2016 Concrete - Complementary British Standard to BS EN 206 Part 1: Method of specifying and guidance for the specifier, *British Standards Institution*, London.

Khalil, M.A. and Santos, F.A.M. (2009). Influence of degree of saturation in the electric resistivity – hydraulic conductivity relationship. *Surveys in Geophysics*. 30, 601-615, 2009. doi:10.1007/s10712-009-9072-4

Li S. and Roy D. M. (1986) Investigation of relations between porosity, pore structure, and $C1^-$ diffusion of fly ash and blended cement pastes. *Cement and Concrete Research.* 16(5), 749-759. doi:10.1016/0008-8846(86)90049-9

Li, Y-H. and Gregory, S. (1974). Diffusion of ions in sea-water and in deep-sea sediments, *Geochimica et Cosmochimica Acta*, 38, 703-714. doi:10.1016/0016-7037(74)90145-8

Long, A.E., Henderson G.D. and Montgomery F.R. (2001). Why assess the properties of near-surface concrete. *Construction and Building Materials*. 15(2/3), 65-79. doi:10.1016/S0950-0618(00)00056-8

Lu, S., Landis, E. N. and Keane, D. T. (2006). X-ray microtomographic studies of pore structure and permeability in Portland cement concrete. *Materials and Structures*. 39(6), 611-620. doi:10.1617/s11527-006-9099-7

McCarter, W. J. and Vennesland, Ø. (2004). Sensor systems for use in reinforced concrete structures. *Construction and Building Materials*, 18(6), 351–358. doi:10.1016/j.conbuildmat.2004.03.008

McCarter, W.J., Chrisp, T.M. and Starrs, G., A sensor apparatus and method for embedding in construction material, Patent No. GB2487691 and WO/2011048378, 2011. https://patentscope.wipo.int/search/en/detail.jsf?docId=WO2011048378&recNum=1&maxRec=&office=&prevFilter=&sortOption=&queryString=&tab=PCT+Biblio

Merioua, A., Bezzar, A. and Ghomari, F. (2015). Non-destructive Electrical Methods for Measuring the Physical Characteristics of Porous Materials. *Journal of Nondestructive Evaluation*, 34(2), Article 13 (12pp). doi:10.1007/s10921-015-0287-7

Muigai, R. , Moyo, P. and Alexander, M. (2012). Durability design of reinforced concrete structures: a comparison of the use of durability indexes in the deemed-to-satisfy approach and the full-probabilistic approach. *Materials and Structures*. 45(8), 1233-1244. doi:10.1617/s11527-012-9829-y

Neithalath, N., Persun, J. and Manchiryal, R.K. (2010). Electrical conductivity based microstructure and strength prediction of plain and modified concretes. *International Journal of Advances in Engineering Sciences and Applied Mathematics.* 2(3), 83–94. doi: 10.1007/s12572-011-0023-1

New Civil Engineer. (2000, May 25). The state of the nation. *New Civil Engineer*. 15-17.

Nganga, G., Alexander, M. and Beushausen, H. (2015) Practical implementation of the durability index performance-based design approach. *Construction and Building Materials*, 45, 251-261. doi:10.1016/j.conbuildmat.2013.03.069

Scherer, G.W., Valenza J.J. and Simmons G. (2007). New methods to measure liquid permeability in porous materials, *Cement and Concrete Research*. 37(3), 386-397. doi:10.1016/j.cemconres.2006.09.020

Shackleford, C. D. and Daniel, D. E. (1991). Diffusion in Saturated Soil. I: Background. *Journal of Geotechnical Engineering*. 117(3), 467-484. doi:10.1061/(ASCE)0733-9410(1991)117:3(467)

Shi, C., Stegemann, J. A. and Caldwell, R. J. (1998). Effect of Supplementary Cementing Materials on the Specific Conductivity of Pore Solution and its Implications on the Rapid Chloride Permeability Test (AASHTO T277 and ASTM C1202) Results. *ACI Materials Journal*. 95(4), 389-394

Snyder, K.A., Feng, X., Keen, B.D. and Mason, T.O. (2003). Estimating the electrical conductivity of cement paste pore solutions from OH^-, K^+ and Na^+ concentrations. *Cement and Concrete Research.* 33(6), 793-798. doi:10.1016/S0008-8846(02)01068-2

Spragg, R., Bu, Y., Snyder, K., Bentz, D. and Weiss, J. (2013). Electrical Testing of Cement-Based Materials: Role of Testing Techniques, Sample Conditioning, and Accelerated Curing. *Publication FHWA/IN/JTRP-2013/28*. Joint Transportation Research Program, Indiana Department of Transportation and Purdue University, West Lafayette, Indiana. doi:10.5703/1288284315230

Swamy, R.N. (2008, April). Holistic Design: Key to Sustainability in Concrete Construction. *JSCE Concrete Committee.* Newsletter No. 13. Retrieved from: http://www.jsce.or.jp/committee/concrete/e/newsletter/newsletter13/newsletter13.asp

Taylor, H.F.W. (1987). A method for predicting alkali ion concentrations in cement pore solutions, *Advances in Cement Research*. 1(1), 5-16. doi:10.1680/adcr.1987.1.1.5

Tutti, K. (1982). Corrosion of Steel in Concrete, Report Fo 4.82, Swedish Cement and Concrete Association, Stockholm, pp469. Retrieved from: http://portal.research.lu.se/portal/files/4709458/3173290.pdf#page=34&zoom=auto,-120,519 (accessed 12/01/2017)

Worthington, P.F. (1993). The uses and abuses of the Archie equations, 1: the formation factor – porosity relationship. *Journal of Applied Geophysics*. 30(3), 215-228. doi:10.1016/0926-9851(93)90028-W

Captions for Figures

Fig. 1 Components of service life.

Fig. 2 (a) Electrode array embedded within slab samples for long-term testing, and (b) experimental set-up for long-term testing.

Fig. 3 Resistivity during initial 24-hours for (a) PC concretes, (b) GGBS/65 concretes, and (c) FA/35 concretes.

Fig. 4 Variation in resistivity for electrode-pairs at 10, 20, 30 and 75mm from the concrete surface undergoing cyclic wetting (PC concrete, w/b=0.65).

Fig. 5 Increase in resistivity during initial 28-days after casting for concretes (a) w/b=0.35 and (b) w/b=0.65.

Fig. 6 Increase in resistivity over the period 7-350 days after casting for concretes (a) w/b = 0.35 and (b) w/b = 0.65. Curve fits in the form of equation (5) are also presented.

Fig. 7 Curve-fits (solid lines) to concrete resistivity measurements based on 3 (three) measurement points – 7, 28 and 56 days for (a) w/b = 0.35 and (b) w/b = 0.65. Curve fits based on all measurements points indicted with dashed lines.

Fig. 8 Pore-fluid resistivity, ρ_p, for all cementitious binders evaluated using the work of Snyder, Feng, Keen and Mason (2003) and Bentz (2007).

Table 1 Summary of concrete mixes (pl =plasticiser, w/b = water-binder ratio, FA = fly ash, GGBS = ground granulated blast-furnace slag). Figure in brackets is standard deviation for compressive strength results.

Mix	w/b	CEM I kg/m^3	GGBS kg/m^3	FA kg/m^3	20mm kg/m^3	10mm kg/m^3	Fine (<4mm) kg/m^3	pl l/m^3	f_{28} MPa	f_{180} MPa
PC	0.35	378	-	-	787	393	787	5.15	79 (0.95)	88 (1.44)
	0.65	263	-	-	790	395	790	-	39 (0.87)	46 (2.52)
GGBS/65	0.35	132	244	-	782	391	782	5.12	65 (2.26)	76 (0.58)
	0.65	92	170	-	786	393	786	-	31 (0.79)	40 (2.31)
FA/35	0.35	242	-	130	773	386	773	5.06	65 (0.38)	81 (1.15)
	0.65	169	-	91	780	390	780	-	24 (0.35)	38 (0.95)

Table 2 Oxide analysis of cementitious materials used in experimental programme.

% by weight	PC	FA	GGBS
SiO_2	20.68	51.0	34.33
Al_2O_3	4.83	27.4	12.60
Fe_2O_3	3.17	4.6	0.60
CaO	63.95	3.4	41.64
MgO	2.53	1.4	8.31
TiO_2	+	1.6	+
P_2O_5	+	0.3	+
SO_3	2.80	0.7	+
K_2O	0.54	1.0	0.47
Na_2O	0.08	0.2	0.25

+ not determined

Table 3 Formation factors (F) for the concrete mixes in Table 1 at 28-days (F_{28}) and 56-days (F_{56}). Note: the figure in brackets is the standard deviation for the value presented.

Mix	w/b	ρ_p* (Ωcm)	ρ_{28} ($\times 10^4$ Ωcm)	ρ_{56} ($\times 10^4$ Ωcm)	F_{28}	F_{56}
PC	0.35	10.7	0.725 (0.032)	0.865 (0.037)	677 (30)	808 (34)
	0.65	23.6	0.368 (0.030)	0.445 (0.034)	156 (12)	188 (14)
GGBS/65	0.35	27.8	3.23 (0.210)	4.46 (0.275)	1162 (75)	1604 (100)
	0.65	57.6	1.69 (0.110)	2.32 (0.153)	293 (19)	403 (27)
FA/35	0.35	8.31	0.952 (0.045)	2.01 (0.093)	1146 (54)	2419 (112)
	0.65	18.1	0.394 (0.031)	0.842 (0.066)	218 (17)	465 (37)

* calculated value

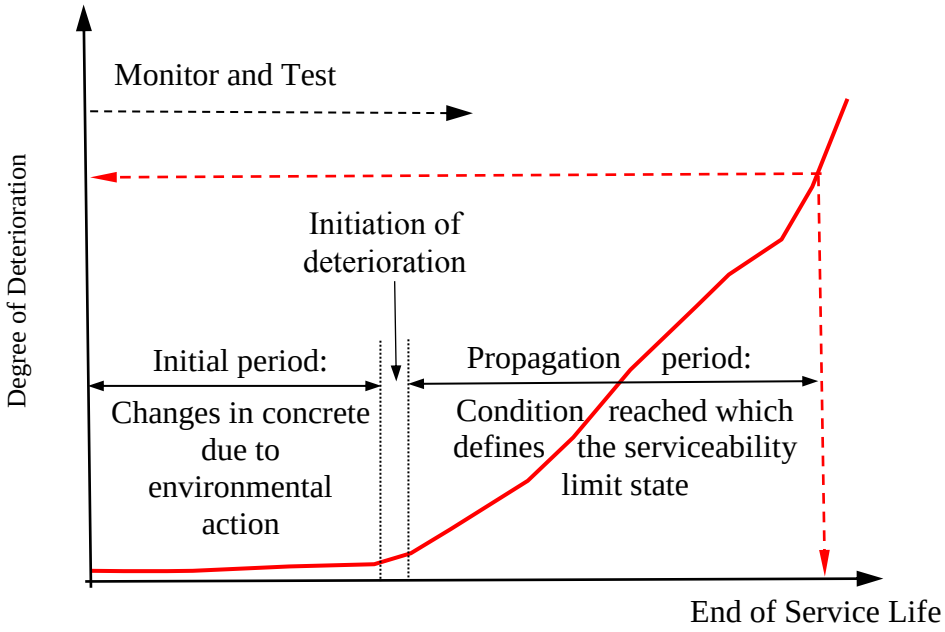
Monitor and Test
Degree of Deterioration
Initiation of deterioration
Initial period:
Changes in concrete due to environmental action
Propagation period:
Condition reached which defines the serviceability limit state
End of Service Life

Figure 1

Figure 2(a)

Figure 2(b)

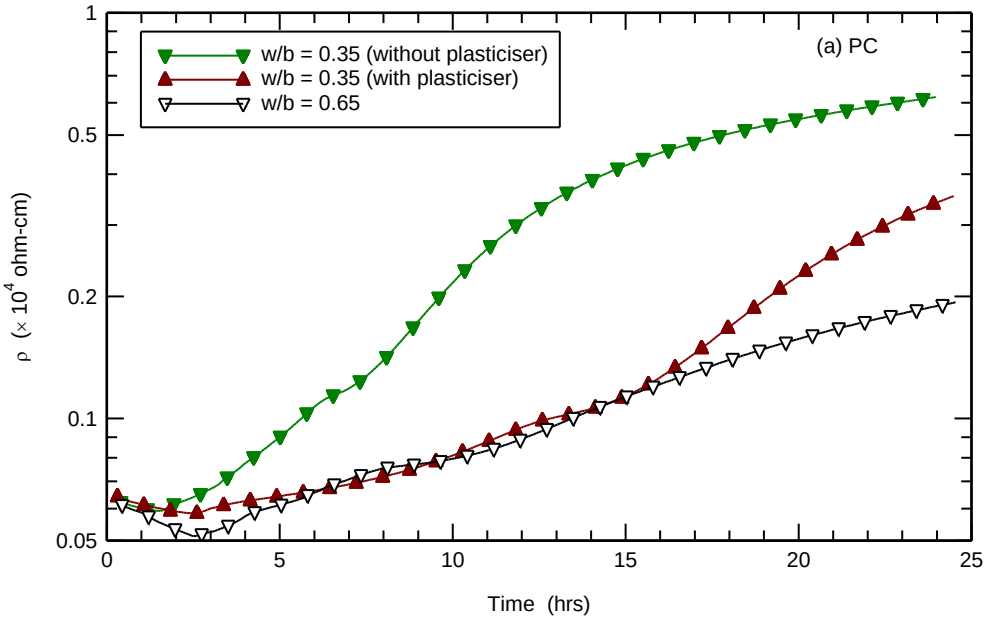
w/b = 0.35 (without plasticiser)
w/b = 0.35 (with plasticiser)
w/b = 0.65
(a) PC
ρ (× 10^4 ohm-cm)
Time (hrs)
1
0.5
0.2
0.1
0.05
0
5
10
15
20
25

Figure 3(a)

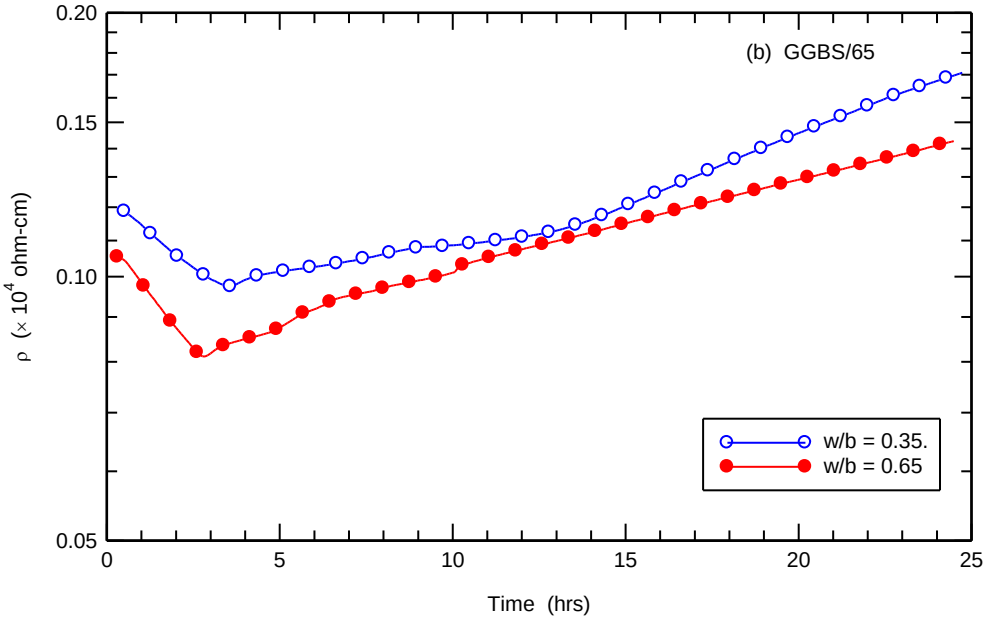
(b) GGBS/65
w/b = 0.35.
w/b = 0.65
ρ (× 10^4 ohm-cm)
Time (hrs)
0.20
0.15
0.10
0.05
0
5
10
15
20
25

Figure 3(b)

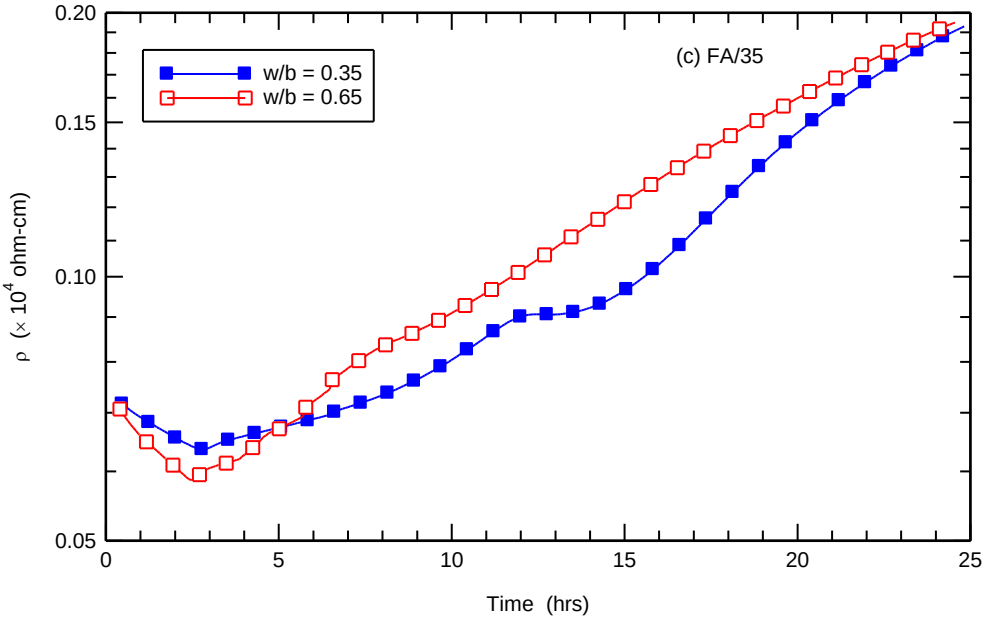
(c) FA/35
w/b = 0.35
w/b = 0.65
ρ (× 10^4 ohm-cm)
Time (hrs)
0.20
0.15
0.10
0.05
0
5
10
15
20
25

Figure 3(c)

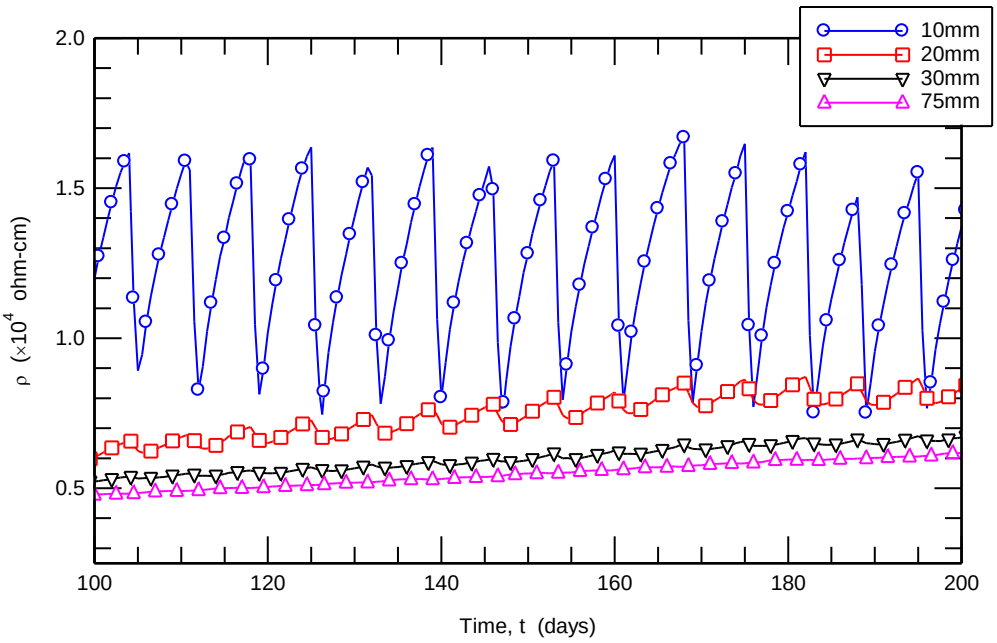
10mm
20mm
30mm
75mm
2.0
1.5
1.0
0.5
ρ (×10^4 ohm-cm)
100
120
140
160
180
200
Time, t (days)

Figure 4

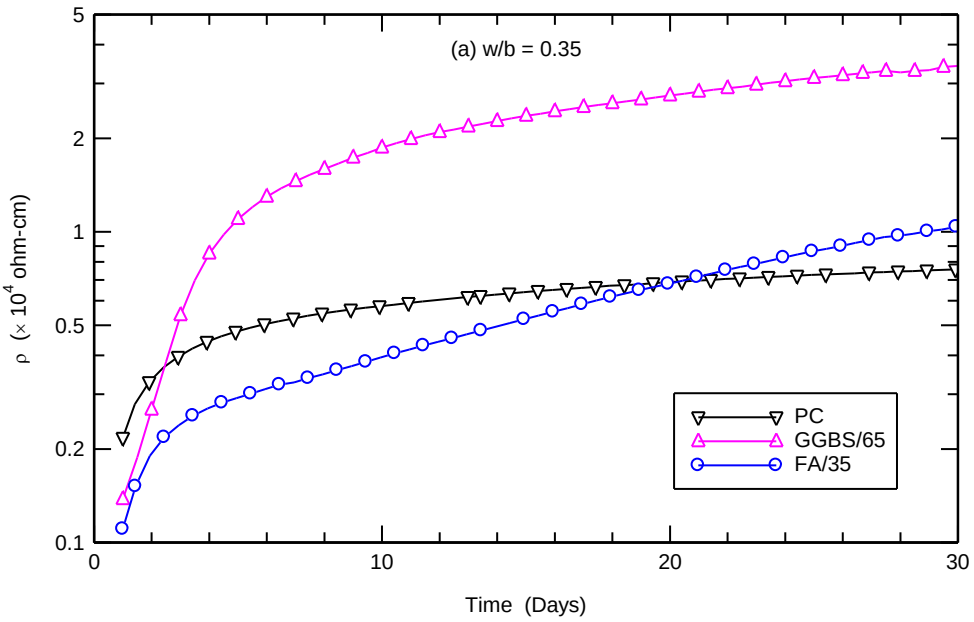
(a) w/b = 0.35
ρ (× 10^4 ohm-cm)
Time (Days)
PC
GGBS/65
FA/35
5
2
1
0.5
0.2
0.1
0
10
20
30

Figure 5(a)

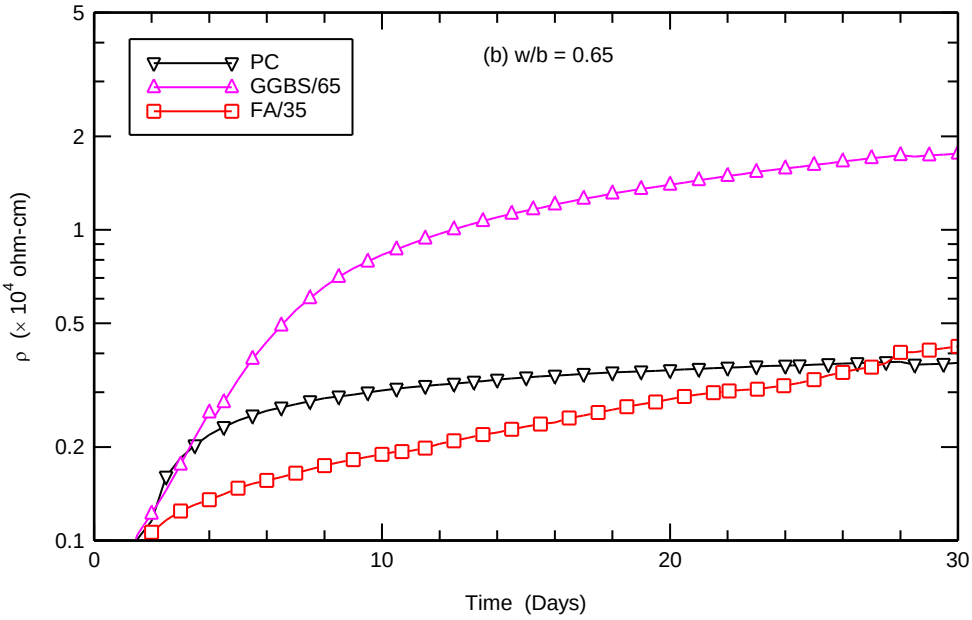
(b) w/b = 0.65
PC
GGBS/65
FA/35
ρ (× 10^4 ohm-cm)
Time (Days)
5
2
1
0.5
0.2
0.1
0
10
20
30

Figure 5(b)

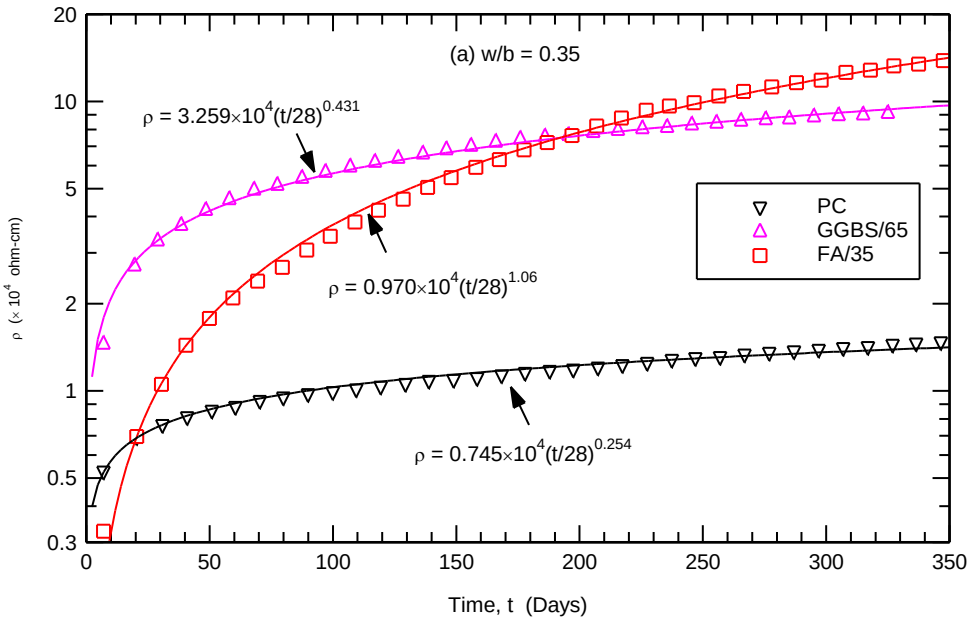
(a) w/b = 0.35
ρ = 3.259×10^4(t/28)^0.431
ρ = 0.970×10^4(t/28)^1.06
ρ = 0.745×10^4(t/28)^0.254
PC
GGBS/65
FA/35
ρ (× 10^4 ohm-cm)
Time, t (Days)
20
10
5
2
1
0.5
0.3
0
50
100
150
200
250
300
350

Figure 6(a)

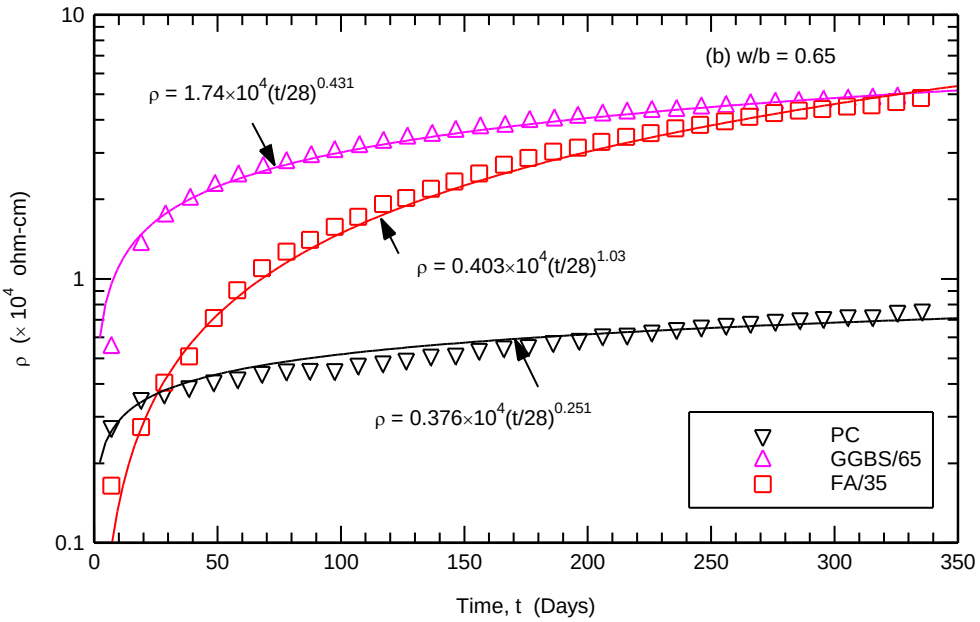
(b) w/b = 0.65
ρ = 1.74×10^4(t/28)^0.431
ρ = 0.403×10^4(t/28)^1.03
ρ = 0.376×10^4(t/28)^0.251
PC
GGBS/65
FA/35
ρ (× 10^4 ohm-cm)
Time, t (Days)
10
1
0.1
0
50
100
150
200
250
300
350

Figure 6(a)

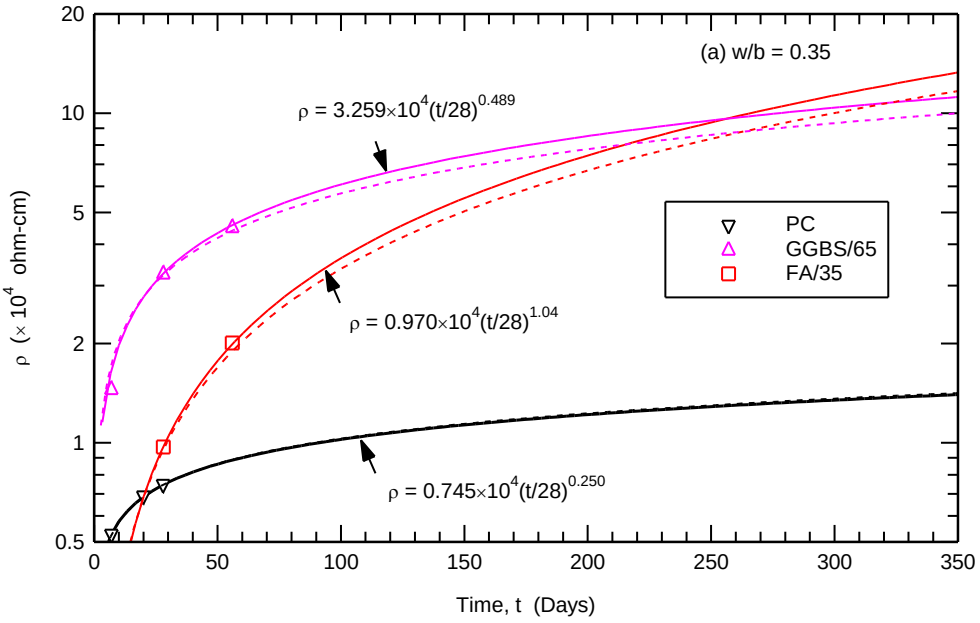
(a) w/b = 0.35
ρ = 3.259×10^4(t/28)^0.489
ρ = 0.970×10^4(t/28)^1.04
ρ = 0.745×10^4(t/28)^0.250
PC
GGBS/65
FA/35
ρ (× 10^4 ohm-cm)
Time, t (Days)
20
10
5
2
1
0.5
0
50
100
150
200
250
300
350

Figure 7(a)

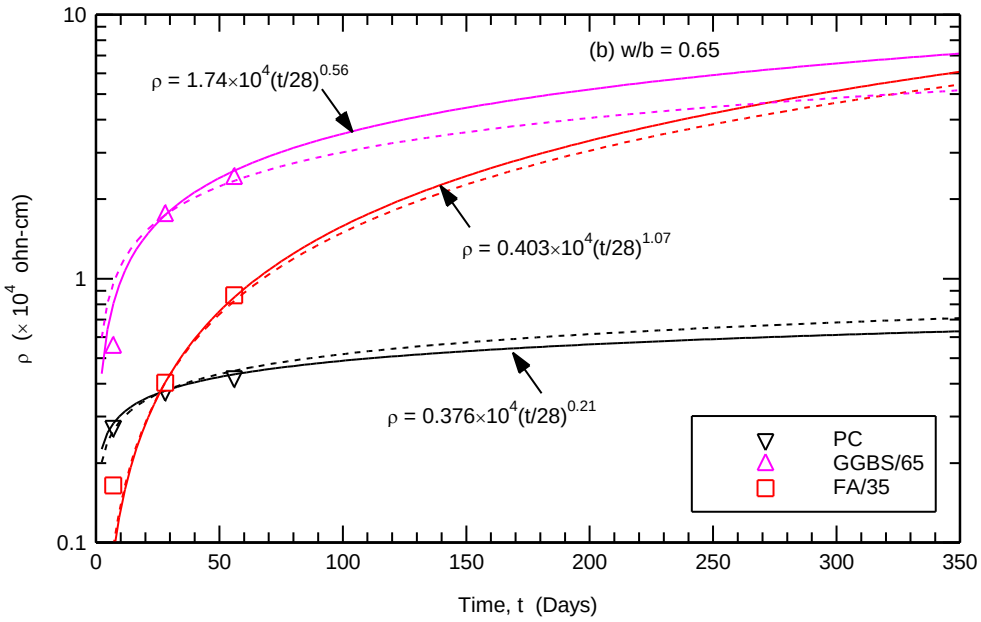
(b) w/b = 0.65
ρ = 1.74×10^4(t/28)^0.56
ρ = 0.403×10^4(t/28)^1.07
ρ = 0.376×10^4(t/28)^0.21
PC
GGBS/65
FA/35
ρ (× 10^4 ohm-cm)
Time, t (Days)
10
1
0.1
0
50
100
150
200
250
300
350

Figure 7(b)

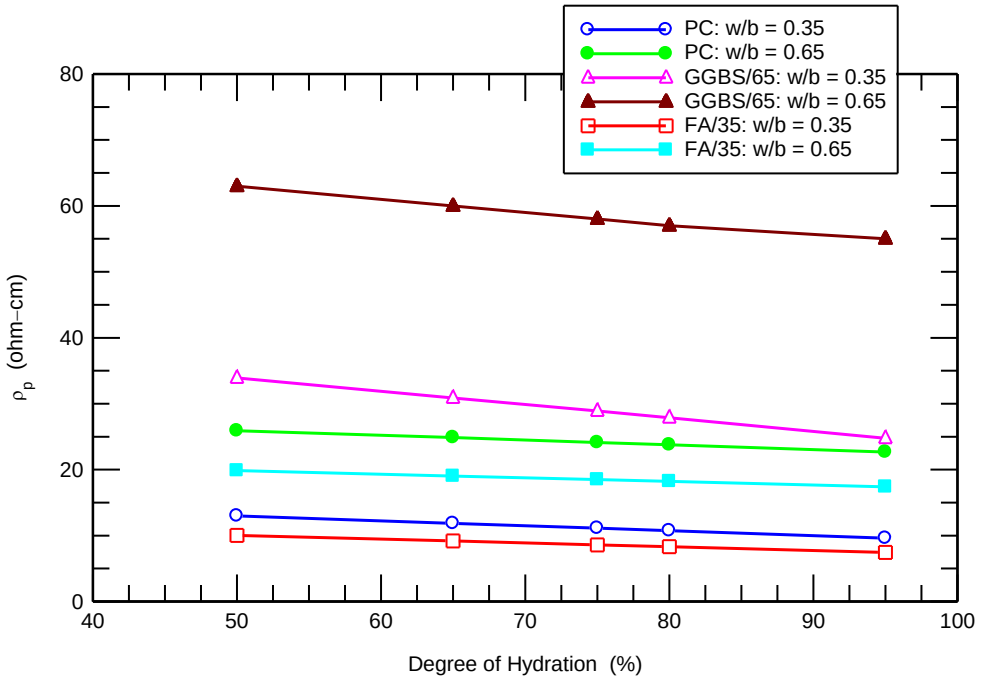
PC: w/b = 0.35
PC: w/b = 0.65
GGBS/65: w/b = 0.35
GGBS/65: w/b = 0.65
FA/35: w/b = 0.35
FA/35: w/b = 0.65
80
60
40
20
0
40
50
60
70
80
90
100
ρp (ohm–cm)
Degree of Hydration (%)

Figure 8